The Oncologist, 2023, **28**, e1031–e1042
https://doi.org/10.1093/oncolo/oyad113
Advance access publication 9 May 2023
Original Article

Association of Tumor Cell Metabolic Subtype and Immune Response With the Clinical Course of Hepatocellular Carcinoma

Xiaolin Wei[1,‡], Theodoros Michelakos[2,‡], Qian He[1,‡], Xianxing Wang[3], Yu Chen[4], Filippos Kontos[2], Huaizhi Wang[3], Xiangde Liu[1], Hui Liu[1], Wenjing Zheng[1], Soldano Ferrone[2,†], Yun Zhang[5], Cristina R. Ferrone[*,2,6], Xiaowu Li[*,1], Lei Cai[*,3]

[1]Department of Hepatobiliary Surgery, Shenzhen University General Hospital & Guangdong Provincial Key Laboratory of Regional Immunity and Diseases and Carson International Cancer Shenzhen University General Hospital and Shenzhen University Clinical Medical Academy Center, Shenzhen University, Shenzhen, People's Republic of China
[2]Department of Surgery, Massachusetts General Hospital, Harvard Medical School, Boston, MA, USA
[3]Institute of Hepatopancreatobiliary Surgery, Chongqing General Hospital, University of Chinese Academy of Sciences, Chongqing, People's Republic of China
[4]Department of Digestive Diseases, Shanghai Fourth People's Hospital Affiliated to Tongji University, Shanghai, People's Republic of China
[5]Department of Foreign Languages, Army Medical University, Chongqing, People's Republic of China
[6]Department of Surgery, Cedar-Sinai Health System, Los Angeles, CA, USA

*Corresponding author: Lei Cai, MD, PhD, Institute of Hepatopancreatobiliary Surgery, Chongqing General Hospital, University of Chinese Academy of Sciences, Chongqing, People's Republic of China. Tel: +8618623360599; Fax: +(0755)21839000; Email: cailei@rocketmail.com; or, Xiaowu Li, MD, PhD, Department of Hepatobiliary Surgery, Shenzhen University General Hospital & Guangdong Provincial Key Laboratory of Regional Immunity and Diseases & Carson International Cancer Shenzhen University General Hospital and Shenzhen University Clinical Medical Academy Center, Shenzhen University, Shenzhen, People's Republic of China. Tel: +8613883065936; Fax: +(0755)21839000; Email: lixw1966@163.com; or, Cristina R. Ferrone, MD, Department of Surgery, Cedars-Sinai Health System, 8700 Beverly Boulevard, North Tower STE 8215, Los Angeles, CA 90048, USA. Tel: +13102488156; Email: Cristina.Ferrone@cshs.org
[†]Deceased.
[‡]Contributed equally

Abstract

Aim: Tumor metabolism plays an important role in tumorigenesis and tumor progression. This study evaluated the potential association of tumor cell metabolism and immune cell tumor infiltration with the clinical course of hepatocellular carcinoma (HCC).

Methods: Gene-wise normalization and principal component analysis were performed to evaluate the metabolic system. A tumor microenvironment score system of tumor immune cell infiltration was constructed to evaluate its association with metabolic subtypes. Finally, we analyzed the impact of metabolism and immune cell infiltration on the clinical course of HCC.

Results: A total of 673 HCC patients were categorized into cholesterogenic (25.3%), glycolytic (14.6%), mixed (10.4%), and quiescent (49.8%) types based on glycolysis and cholesterol biosynthesis gene expression. The subgroups including the glycolytic genotyping expression (glycolytic and mixed types) showed a higher mortality rate. The glycolytic, cholesterogenic, and mixed types were positively correlated with M0 macrophage, resting mast cell, and naïve B-cell infiltration ($P = .013$, $P = .019$, and $P = .006$, respectively). In TCGA database, high $CD8^+$ T cell and low M0 macrophage infiltration were associated with prolonged overall survival (OS, $P = .0017$ and $P < .0001$, respectively). Furthermore, in glycolytic and mixed types, patients with high M0 macrophage infiltration had a shorter OS ($P = .03$ and $P = .013$, respectively), and in quiescent type, patients with low naïve B-cell infiltration had a longer OS ($P = .007$).

Conclusions: Tumor metabolism plays a prognostic role and correlates with immune cell infiltration in HCC. M0 macrophage and $CD8^+$ T cell appear to be promising prognostic biomarker for HCC. Finally, M0 macrophages may represent a useful immunotherapeutic target in patients with HCC.

Key words: hepatocellular carcinoma; metabolic reprogramming; immune microenvironment; programmed cell death-Ligand 1(PD-L1); macrophage.

Implications for Practice

Hepatocellular carcinoma (HCC) is one of the most common malignancies. The Barcelona Clinic Liver Cancer (BCLC) staging is used widely, but its value is limited. The molecular events of HCC are highly heterogeneous. This study evaluated the potential association of tumor cell metabolic subtype, host's immune response with the clinical course of HCC. The glycolytic, cholesterogenic, and mixed types were positively correlated with M0 macrophage, resting mast cell, and naïve B-cell infiltration. Mixed and glycolytic type were associated with worse overall survival (OS). High CD8+ T cell and low M0 macrophage infiltration were associated with prolonged OS. Furthermore, in glycolytic and mixed types, patients with high M0 macrophage infiltration had a shorter OS. The association of M0 macrophage infiltration with poor prognosis suggests that M0 macrophage-targeting strategies may be beneficial in patients with HCC.

Received: 8 October 2022; Accepted: 15 March 2023.

Introduction

Hepatocellular carcinoma (HCC) is the third leading cause of cancer-related death worldwide.[1] The Barcelona Clinic Liver Cancer (BCLC) staging is widely used as a predictive model, but some patients with early BCLC stages have poor prognoses despite undergoing surgical resection.[2] Sensible prognostic factors are needed to improve the stratification of HCC patients.

The tumor cell metabolic machinery, besides its role in modulating tumor invasiveness, may also affect the host immune response. The glycolytic activity provides an inherent growth advantage for tumor cells and has tumor cell-extrinsic effects that abrogate tumor immunosurveillance.[3] Inhibition of tumor cell glycolysis enhances the generation of memory recognition ability of $CD8^+$ T cells and their anti-tumor effects.[4] Recent studies have shown that lipid metabolism disorders of liver cells lead to $CD4^+$ T-cell exhaustion mediated by reactive oxygen species and promote tumor progression in HCC.[5] Glycolysis, tricarboxylic acid cycle, and fatty acid metabolism can modulate macrophage functions through cytokines, phagocytosis, or antigen presentation.[6] However, the robust evidence of the role of metabolism, immune response, and their interplay and how each tumor cell metabolic status might influence the immune microenvironment is barely understood in HCC.

The objectives of this study using database analysis were to (1) identify the metabolic subtypes in HCC; (2) analyze immune cell infiltration, PD-1, and PD-L1 expression, as well as their correlation with metabolic subtypes in HCC; and (3) assess the clinical relevance of the metabolic subtypes and immune system components by correlating them with clinicopathologic parameters and survival in HCC patients. The resulting information is expected to contribute to the identification of potential metabolic and immune targets of immunotherapeutic strategies for HCC.

Materials and Methods

TCGA (LIHC-US) and ICGC (LICA-FR, LIRI-JP) Expression Profile Data

Standardized RNA-Seq reads (Release 28) of 3 HCC projects were obtained from The Cancer Genome Atlas (TCGA) and International Cancer Genome Collaboration (ICGC),[7] including LICA-FR (n = 161), LIHC-US (n = 292), and LIRI-JP (n = 220), adding to a total of 673 samples. Based on the sample annotations provided by ICGC, only samples from the primary site were included in the analysis. For LIHC-US (TCGA), only one technical repeat was retained, and its standardized expression profile was converted to Transcripts Per Kilobase of exon model per Million mapped reads (TPM).

Obtaining and Pre-Processing GEO Verification Data

The GSE14520[8] chip data were obtained from the GEO database, from which tumor samples (HG-U133A platform) were extracted, consisting of a total of 225 samples. Since a total of 247 samples was contained in 2 platforms, HG-U133A (n = 225) and HG-U133a2 (n = 22) but the latter cohort had a small sample size. Thus, the power of the latter cohort for batch correction was considered limited and excluded from further analysis. The chip data were standardized based on a robust multichip average method. The expression value of the gene was calculated based on the correspondence between the probe and the gene. In cases of one gene corresponding to multiple probes, we used the average of these probes as the expression value of the gene.

The workflow of this study is shown in Supplementary Fig. S1.

Results

Clinicopathologic Features

The median age of the 673 patients with HCC was 61 years (range 18-90), 221 (24.1%) patients were female, 270 (29.5%) tumors were TNM grade T1, 252 (27.5%) T2, 180 (19.6%) T3, and the remaining 31 (3.4%) T4 at diagnosis. One hundred sixty (17.5%) patients had serum Alpha-fetoprotein (AFP) > 300 ng/mL (Table 1).

Distribution of Metabolic Types, Metabolism-Related Gene Mutations, and MPC Expression in HCC

Classification of HCC in Four Metabolic Subgroups Based on the Expression of Metabolic Genes

Bioinformatic analysis of 673 HCC patients from TCGA (n = 292) and ICGC (LICA-FR, n = 161; LIRI-JP, n = 220) was conducted. A gene-wise batch correction was performed to completely correct the batch effect difference of the data (Supplementary Fig. S2A, S2B). Then we performed metabolic typing based on the reactome gene sets as "glycolysis" (72 genes) and "cholesterol biosynthesis" (25 genes). Genes were clustered into 3 classes based on changes in consensus coding sequence (CDS) and the area under CDS curves (Supplementary Fig. S3). The extracted glycolysis and cholesterol biosynthesis signatures contained 56 and 18 genes, respectively. Based on the median expression of the signature genes, samples were divided into 4 metabolic subtypes (Fig. 1A), which were cholesterogenic (25.3%), glycolytic (14.6%), mixed (10.4%), and quiescent (49.8%). The heat map of glycolysis and cholesterol biosynthesis gene expression in each metabolic type is shown in Fig. 1B.

Characteristic Blueprint of Metabolic Signature Gene Mutations in the HCC Metabolic Subgroups of TCGA

Seventy-four signature mutations were involved in metabolism-related pathways with a low overall mutation ratio in patients' samples (<4%; Fig. 1C). Moreover, in glycolytic subtypes, ratio of silent mutations in metabolic genes was significantly lower than in mixed and quiescent subtypes (Fig. 1D), and the ratio of non-synonymous mutations did not significantly differ among metabolic subtypes (Fig. 1E).

Association of Metabolic Subtypes and Mutated Metabolism-Related Genes in HCC

The genes with the highest mutation ratio were *Titin* (*TTN*, 29%), *Catenin beta-1* (*CTNNB1,* 25%), and *Tumor protein p53* (*TP53*, 23%) (Fig. 2A). No significant difference in gene mutation distribution was observed among 4 subtypes. Subsequently, *TTN* mutation positively correlated with cholesterol biosynthesis (Spearman's correlation test, $P < .001$); *TP53* and *CTNNB1* mutation positively correlated

Table 1. Clinicopathologic features.

	GEO GSE14520 (N=247)	ICGC		TCGA LIHC-US (N=292)	Overall (*N* = 916)
		LICA-FR (N=161)	LIRI-JP (N=216)		
Gender					
Female	31 (12.6%)	34 (21.1%)	58 (26.9%)	98 (33.6%)	221 (24.1%)
Male	211 (85.4%)	127 (78.9%)	158 (73.1%)	194 (66.4%)	690 (75.3%)
N/A	5 (2.0%)	0(0%)	0(0%)	0(0%)	5 (0.5%)
Age (at diagnosis, years)					
Mean (SD)	50.8 (10.9)	63.4 (12.3)	67.6 (9.78)	60.0 (13.0)	60.0 (13.1)
Median [min, max]	50.0 [21.0, 77.0]	66.0 [21.0, 90.0]	69.0 [31.0, 89.0]	61.0 [18.0, 90.0]	61.0 [18.0, 90.0]
N/A	5 (2.0%)	0(0%)	0(0%)	0(0%)	5 (0.5%)
Tumor stage (at diagnosis)					
T1	96 (38.9%)	1 (0.6%)	33 (15.3%)	140 (47.9%)	270 (29.5%)
T2	78 (31.6%)	2 (1.2%)	100 (46.3%)	71 (24.3%)	251 (27.4%)
T2b	0(0%)	0(0%)	0(0%)	1 (0.3%)	1 (0.1%)
T3	3 (1.2%)	0(0%)	65 (30.1%)	33 (11.3%)	101 (11.0%)
T3a	29 (11.7%)	0(0%)	0(0%)	26 (8.9%)	55 (6.0%)
T3b	15 (6.1%)	0(0%)	0(0%)	5 (1.7%)	20 (2.2%)
T3c	4 (1.6%)	0(0%)	0(0%)	0(0%)	4 (0.4%)
T4	0(0%)	0(0%)	18 (8.3%)	13 (4.5%)	31 (3.4%)
TX	0(0%)	0(0%)	0(0%)	1 (0.3%)	1 (0.1%)
N/A	22 (8.9%)	158 (98.1%)	0(0%)	2 (0.7%)	182 (19.9%)
AFP					
AFP ≤ 300 ng/mL	128 (51.8%)	0(0%)	0(0%)	163 (55.8%)	291 (31.8%)
AFP>300 ng/mL	110 (44.5%)	0(0%)	0(0%)	50 (17.1%)	160 (17.5%)
N/A	9 (3.6%)	161 (100%)	216 (100%)	79 (27.1%)	465 (50.8%)

Abbreviations: AFP, alpha-fetoprotein; N/A, not available.

with glycolysis (Spearman's correlation test, $P < .0001$ and $P < .0001$, respectively, Fig. 2B).

The mutation ratios and metabolism-related gene expression in 4 subgroups were compared (Fig. 2C). *MPC1* expression was significantly lower in glycolytic than in cholesterogenic and quiescent subtype (Wilcoxon rank-sum test, cholesterogenic vs. glycolytic, $P = .0015$, glycolytic vs. quiescent, $P = .0058$) and was significantly lower in mixed than in cholesterogenic subtype ($P = .0235$). *MPC2* expression was significantly higher in cholesterogenic than in quiescent subtype (Wilcoxon rank-sum test, $P = .0003$, Fig. 2D).

We also identified *MPC1* and *MPC2* expression-related genes based on Spearman's correlation test (BH-adjusted, $P < .05$), and further investigated the enhancer ($R > 0.25$, $n = 199$) and suppressor genes ($R <– 0.25$, $n = 98$, Fig. 2E) that correlated with *MPC1* and *MPC2* expression. Genes that correlated with upregulated *MPC1* and *MPC2* expression were enriched in a variety of metabolism-related functions. Genes which correlated with downregulated *MPC1* and *MPC2* expression enriched in mitogen-activated protein kinase (MAPK) pathway (hypergeometric test, adjusted $P < .05$, Fig. 2F).

Association of Immune Cell Infiltration, PD-1, PD-L1 Expression, and Metabolic Subtypes in HCC

To quantify the proportion of immune infiltrates in HCC tumors (TCGA), we evaluated the infiltration ratios of 22 types of human immune cells (Fig. 3A). Furthermore, we compared their infiltration among metabolic subtypes (Fig. 3B). The distribution of 4 types of immune cells (naïve B cells, M0 macrophages, resting mast cells, and resting memory $CD4^+$ T cells) showed a significant difference among metabolic subtypes. M0 macrophages showed the highest infiltration (Kruskal-Wallis rank-sum test, $P = .013$), and resting memory $CD4^+$ T cells and resting mast cells showed the lowest infiltration in glycolytic subtype (Kruskal-Wallis rank-sum test, 0.008 and 0.006, respectively). Naïve B cells showed the highest infiltration in mixed subtype (Kruskal-Wallis rank-sum test, $P = .019$).

The TMEscore of the glycolytic type was significantly higher than the other subtypes (Fig. 1F). Significant differences in TME scores among different metabolic subtypes may reflect the immune regulatory functions of metabolism in HCC.

PD-1 and PD-L1 expression showed significant differences among metabolic subtypes (Kruskal-Wallis rank sum test, $P < .05$, Fig. 3C).

Association of Metabolic Subgroups and Immune Cell Infiltration With Clinical Features and Prognosis in HCC

Association of Metabolic Subtypes With MANTIS Score, TNM Classification, and Alpha-Fetoprotein (AFP) Expression

Three samples (1.1%) were classified as MSI-H. To avoid bias due to threshold settings, MANTIS scores were used in this study, but there were no significant differences in

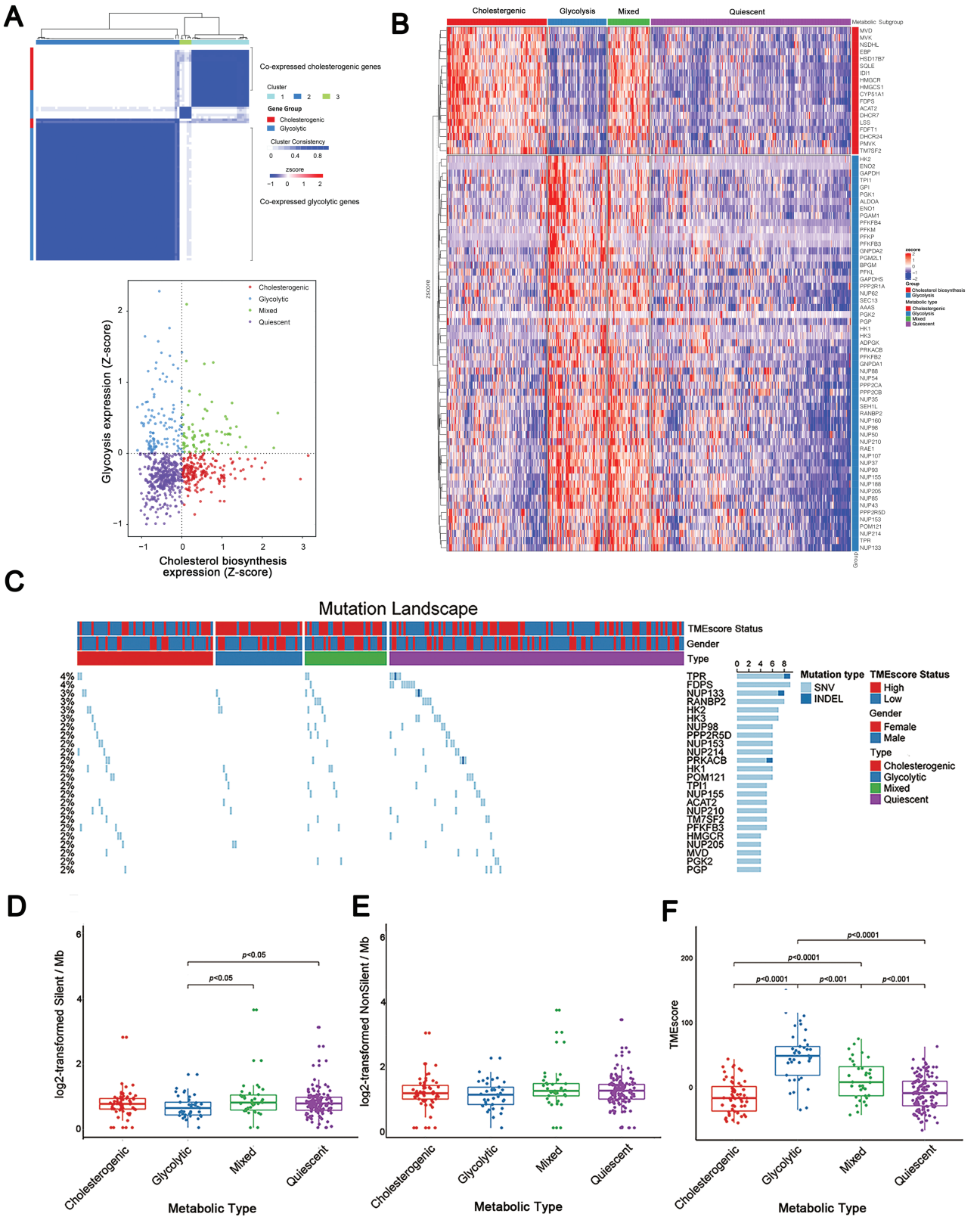

Figure 1. Tumor metabolic types of HCC patients based on the expression of glycolysis and cholesterol biosynthesis genes. (**A**) Identification of signatures of co-expressed glycolysis and cholesterol biosynthesis genes and typing of HCC patients based on consensus clustering. (**B**) Heat map of glycolysis and cholesterol biosynthesis gene expression in each metabolic type. (**C**) Mutations of 24 metabolic pathway genes (only genes with mutation ratio > 2% are displayed) in 4 metabolic subtypes. The bar graph on the right shows the ratio of mutation of each gene. Each column represents a patient, and the upper bar graph indicates the TMEscore grouping (divided into "High" and "Low" group according to the median value), gender, and metabolic type of the patient. (**D**) The ratio of silent mutations in metabolic genes was significantly lower in the glycolytic subtypes than in mixed and quiescent subtypes (Wilcoxon rank sum test, glycolytic vs. mixed, $P < .05$ glycolytic vs. quiescent, $P < .05$). (**E**) The ratio of non-synonymous mutations in metabolic genes did not significantly differ among the 4 metabolic subtypes. (**F**) The TMEscore of the glycolytic type was significantly higher than the cholesterogenic, mixed and quiescent type (Wilcoxon rank sum test, glycolytic vs. cholesterogenic, $P < .0001$, glycolytic vs. mixed, $P < .001$, glycolytic vs. quiescent, $P < .0001$). And the TMEscore of the mixed type was significantly higher than the cholesterogenic and quiescent type (Wilcoxon rank sum test, mixed vs. cholesterogenic, $P < .0001$, mixed vs. quiescent, $P < .001$).

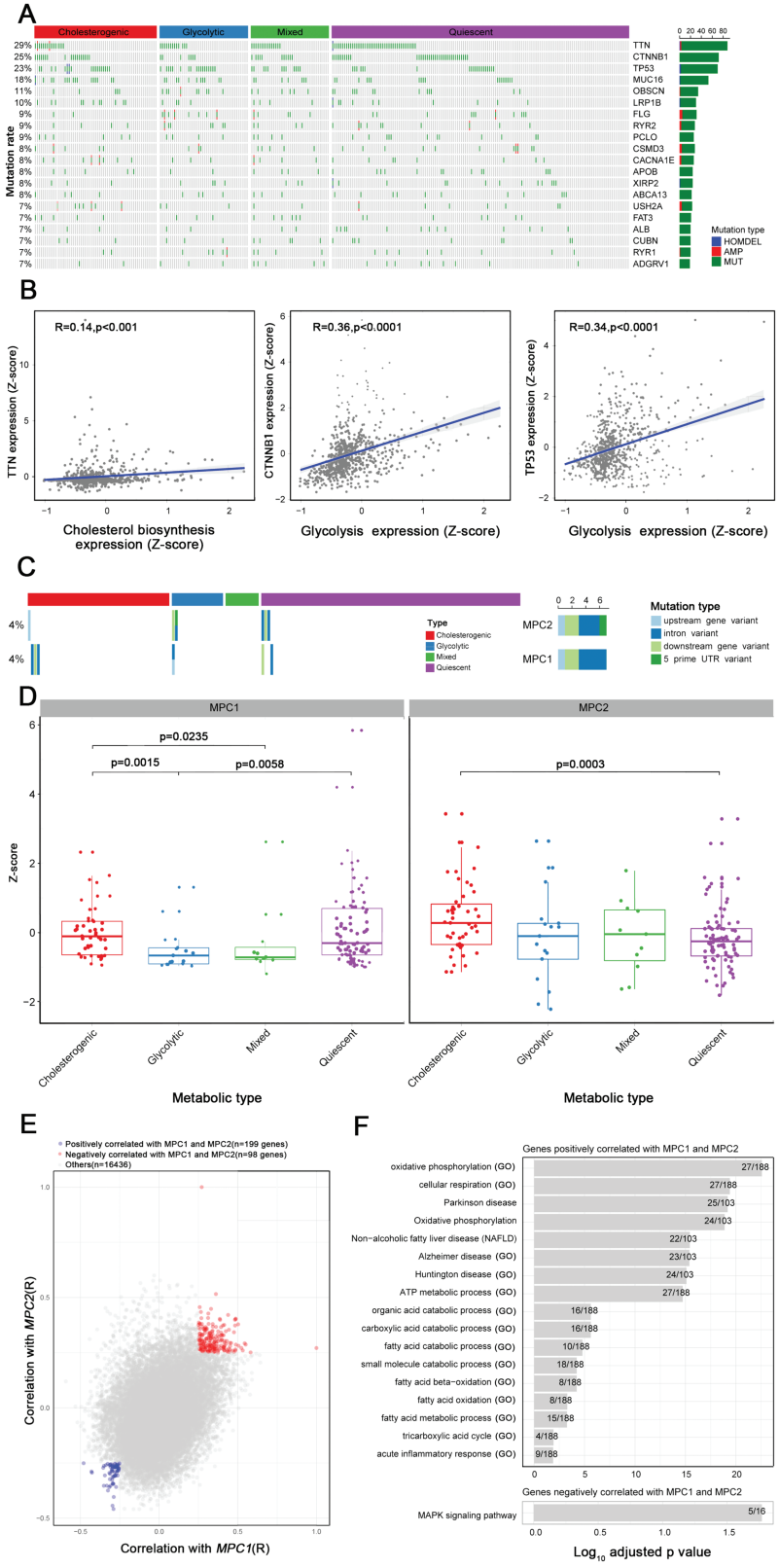

Figure 2. Association of mutated genes, MPC1 and MPC2 expression with metabolic types in HCC. (**A**) The distribution of mutated genes among metabolic types. (**B**) *TTN* mutation was correlated with cholesterol biosynthesis (Spearman's correlation test, $P < .001$), and *TP53* and *CTNNB1* mutation was correlated with glycolysis (Spearman's correlation test, $P < .0001$ and $P < .0001$). (**C**) The distribution of MPC1 and MPC2 genomic alteration events among metabolic types. (**D**) MPC1 gene expression in the glycolytic subtype was significantly lower than in the cholesterogenic and quiescent subtype (Wilcoxon rank-sum test, cholesterogenic vs. glycolytic, $P = .0015$; glycolytic vs. quiescent, $P = .0058$) and MPC2 gene expression were significantly higher in the cholesterogenic subtype than in the quiescent subtype (Wilcoxon rank-sum test, $P = .0003$). (**E**) Scatter plot showing genes related to MPC1 and MPC2 gene expression. (**F**) The most significantly enriched functions of genes that promote (upper) and suppress (lower) MPC1 or MPC2 gene expression.

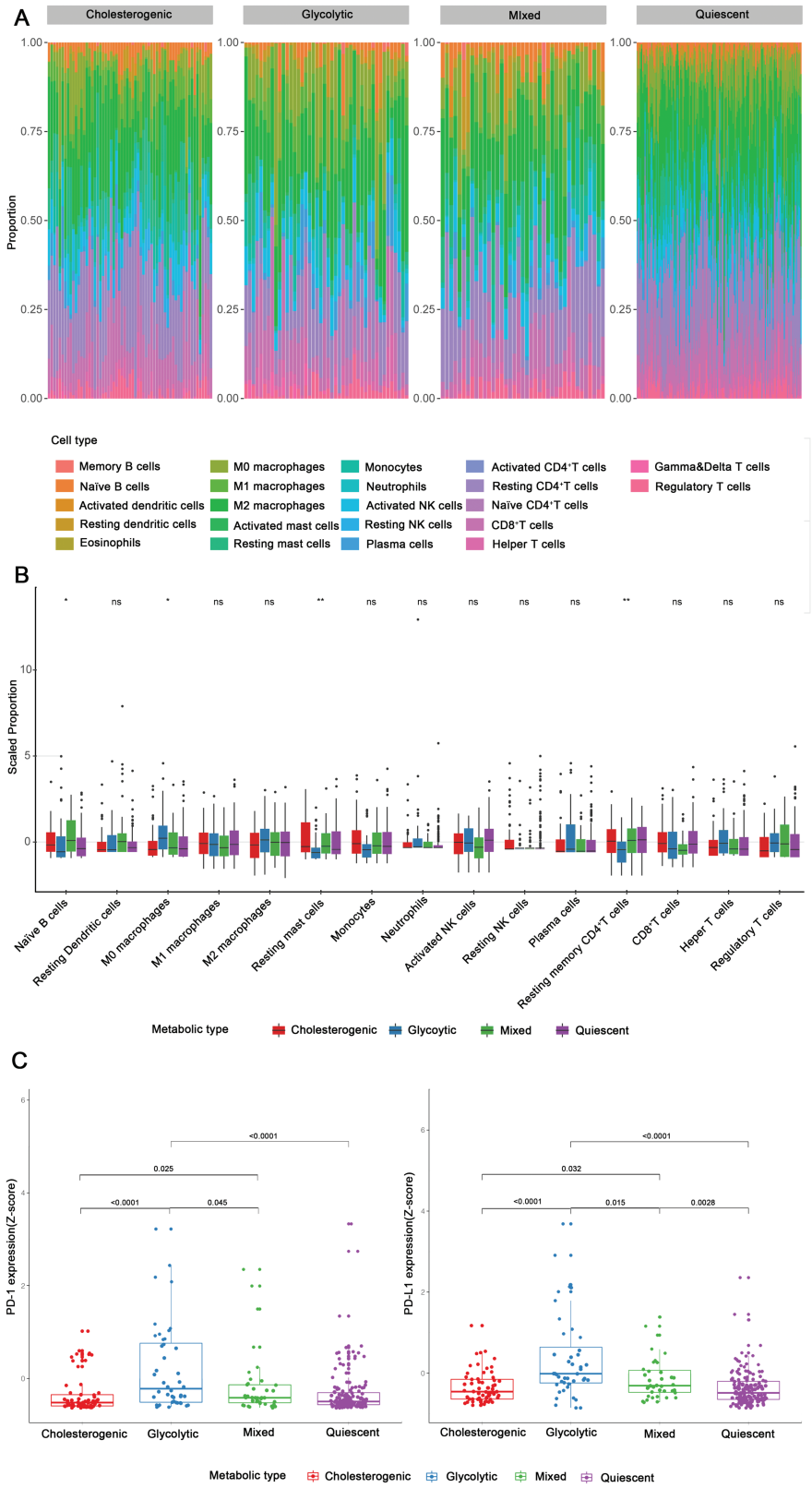

Figure 3. Immune cell infiltration and PD-1/PD-L1 expression by HCC tumors in TCGA-LIHC HCC metabolic subtypes. (**A**) Twenty-two types of immune cells showed different infiltration ratios with metabolic subtypes in TCGA-LIHC. (**B**) Kruskal-Wallis test showed the differentiation of the immune cell infiltration among metabolic subtypes. (**C**) PD-1 and PD-L1 expression was highest in the glycolytic subtype (Kruskal-Wallis rank sum test, $P < .05$) and lower in the cholesterogenic and quiescent subtypes (Kruskal-Wallis rank sum test, $P < .05$ and $P < .05$, respectively) when compared to the glycolytic subtype.

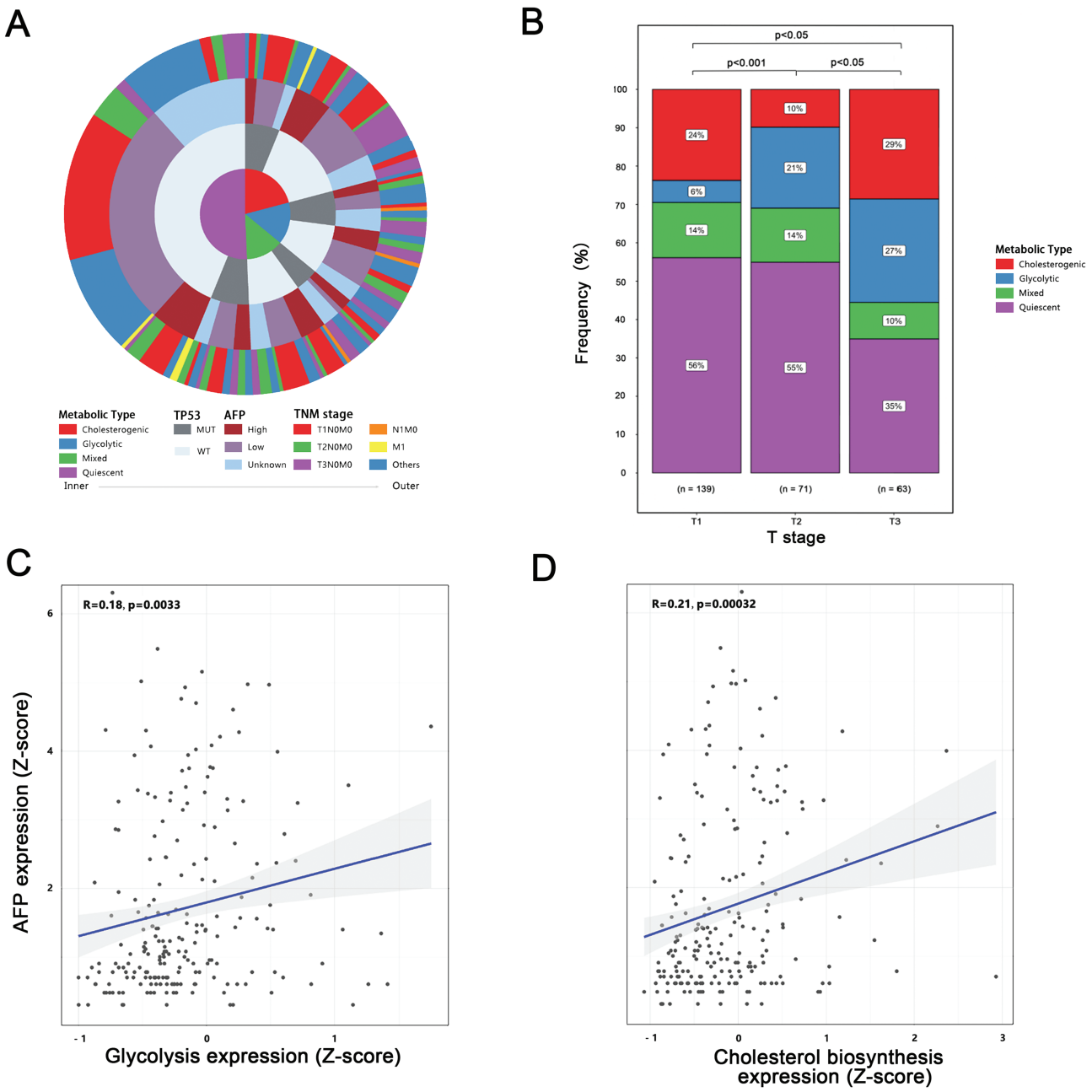

Figure 4. Comparison of HCC metabolic subtypes with TP53 expression, AFP expression and TNM stages. (**A**) Overlay of metabolic profiles (inner loop) with HCC classification methods based on the TP53 expression status, AFP expression and TNM stages (outer rings). (**B**) The distribution of metabolic subtypes was significantly different among different T-stage cohort (Fisher's exact test, TCGA, $P < .001$ for T1 vs. T2, $P < .05$ for T1 vs. T3, and $P < .05$ for T2 vs. T3). (**C**) The expression of glycolysis genes is significantly correlated with AFP expression (Fisher's exact test, $P = .0033$). (**D**) The expression of cholesterol biosynthesis genes is significantly correlated with AFP expression (Fisher's exact test, $P = .00032$).

MANTIS scores among metabolic subtypes and the signature scores of cholesterol biosynthesis and glycolysis ($P > .05$, Supplementary Fig. S4A–S4C).

Furthermore, we analyzed the overlap level between the metabolic subtypes and TNM stages (TCGA, Fig. 4A). The distribution of metabolic subtypes had no significant difference in TNM stages ($P > .05$). However, the distribution of metabolic subtypes had significant difference in T stages (TCGA, $P < .001$ for T1 vs. T2, $P < .05$ for T1 vs. T3 and $P < .05$ for T2 vs. T3, Fig. 4B). Additionally, the quiescent subtypes was associated with lower AFP, and glycolytic and cholesterogenic subtypes were associated with higher AFP (Fisher's exact test, $P < .05$, $P = .0033$, and $P = .00032$, respectively, Fig. 4D, 4E).

Association of Metabolic Subgroups and Host Immune Response With HCC Patients' Survival

Four cases had N/A data and were excluded from survival analysis. In TCGA + ICGC ($n = 511$), median OS in each subtype was: cholesterogenic: 3125 (interquartile range [IQR] 720-not reached [NR]) vs. glycolytic: 1149 (IQR 359-2456) vs. mixed: 810 (IQR 247-NR) vs. quiescent type: 2131 days

(IQR 1088-3258) (P < .0001, Fig. 5A). And 225 cases in GEO and 216 cases in ICGC also confirmed that patients of the mixed subtype had the shortest median OS (GEO: 39.4 months, P = .074; ICGC: 570 days, P = .0006, Supplementary Fig. S5). For HCC patients under 65 years old, similar results with the above were obtained, whereas among patients older than 65 years, the glycolytic subtype showed the highest mortality rate (HR = 2.077, 95%CI = 1.004-4.294, P = .01, Fig. 5B). Since the APF value of HCC patients was only available in TCGA database, we used TCGA to analyze the association of metabolic subtypes and AFP. The results showed that the mixed subtype group had the worst OS among patients with AFP ≤ 300 ng/mL (P = .0015, Fig. 5C). The results above were corroborated with multivariate analyses: metabolic subtype emerged as an independent predictor of survival in TCGA (including age, gender, AFP, and fibrosis as covariates) (HR = 1.489, 95%CI = 1.133-1.958, P = .004), in LIRI-JP (including age, gender, and stage as covariates) (HR = 1.494, 95%CI = 1.091-2.045, P = .012), and in GEO (including AFP as a covariate) (HR = 1.280, 95%CI = 1.015-1.614, P = .037).

Among TCGA (n = 288, 4 cases were showed as N/A in 292 cases), we identified that patients with high M0 macrophage infiltrate (the cutoff of "High/Low" for immune infiltration is the median number, cut-point = 0.338) had a worse prognosis (median OS high = 837 days, IQR 299-2456 vs. low = 2131 days, IQR 770-NR, P < .0001, Fig. 5D). The patients of the cholesterogenic subtype with high M0 macrophage also had a worse prognosis (high vs. low, P = .0029, Fig. 5E). The patients with high $CD8^+$ T cell (cut-point = 0.099) have a better prognosis (median OS high: 617.5 days vs. low: 444 days, P = .00015, Fig. 5D). Furthermore, the patients of the quiescent subtype with high resting mast cell had a better prognosis (HR = 1.1215, 95%CI = 0.8753-1.437, P = .043, Fig. 5F).

In multivariate analyses, both metabolic groups (HR = 1.512, 95%CI = 1.135-2.015, P = .005) and M0 macrophage infiltrates (HR = 1.043, 95%CI = 1.013-1.073, P = .004) emerged as independent predictors of OS.

In TCGA, quiescent subtype patients with low naïve B cell had longer OS (low: 3258 vs. high: 1560 days, P = .0074, Supplementary Fig. S6A). In all of the metabolic subtypes except for mixed subtype, patients with high M0 macrophage demonstrate a shorter OS (cholesterogenic type, high: 581 vs. low: 3125 days, P < .0001; glycolytic type, high: 410 vs. low: 2456 days, P = .0035; quiescent type, high: 1622 vs. low: 2131 days, P = .0043, Supplementary Fig. S6B). In glycolytic and quiescent subtypes, patients with high resting mast cell exhibited shorter survival (glycolytic type, high: 410 vs. low: 2456 days, P = .012; quiescent type, high: 931 vs. low: 2116 days, P = .0096, Supplementary Fig. S6C). The resting memory $CD4^+$ T-cell infiltrates among these 4 subtypes did not show a significant difference in survival (Supplementary Fig. S6D).

The survival of patients with different PD-1 expressions was not different in metabolic subtypes (Supplementary Fig. S7A). However, patients with high PD-1 expression had a marginally longer OS in cholesterogenic subtype (P = .071). Furthermore, patients with high PD-L1 expression had longer OS in glycolytic subtype (high: 1149 days vs. low: 359 days, P = .0024, Supplementary Fig. S7B).

Discussion

Further sub-classifying HCC is important for accurately prognosticating and formulating individualized treatments. Since the metabolism system plays critical role in tumor generation and progression, to analyze the role of glycose, cholestenone, or amino acid and provide useful evidence for the effective cancer metabolic immunotherapy is important. The expression of amino acid metabolism-related genes (AAMRGs) was revealed to predict the prognosis, immune microenvironment, and drug sensitivity of HCC patients.[9] But the role of glycose and cholestenone still lacks related evidence in HCC patients. Herein, HCC patients in TCGA and ICGC were divided into cholesterogenic, glycolytic, mixed, and quiescent subtypes according to the expression of cholesterol and glycolysis biosynthesis genes. Then, we analyzed immune infiltrates which demonstrated that metabolic subtypes are strongly associated with the distribution of immune cells. Furthermore, we investigated the impact of metabolic subtypes and immune cell infiltration on the clinical course of HCC and prognosis of HCC patients.

Our study demonstrated that HCC metabolic subtype is at least partially driven by mutations in oncogenes and tumor suppressor genes. The genes with the highest mutation ratio were *TTN*, *CTNNB1*, and *TP53* (Fig. 2A), and we found *TTN* mutation positively correlated with cholesterol biosynthesis while *TP53* and *CTNNB1* mutation positively correlated with glycolysis (Fig. 2B). In terms of glycolytic metabolism, we detected a high *TP53* mutation rate (23%) in HCC. This is concordant with a related report, demonstrating a *TP53* mutation in ~30% of HCC patients.[10] Moreover, studies have demonstrated that in HCC patients with *TP53* mutation, the development and progression of HCC can be promoted through the tumor cell metabolic phenotype-Warburg effect.[11] In breast cancer, *TP53* mutation is positively correlated with glycolysis, affecting tumor progression.[12] These findings may indicate that *TP53* mutation promotes glycolysis and thus modifies the tumor cell behavior. We also found that *CTNNB1* had a high mutation ratio (25%). This mutation promotes glycolysis and enhances HCC cell proliferation by regulating ALDOA phosphorylation.[13] It also positively correlated with metabolic status such as cholestasis in HCC,[14] making CTNNB1 expression a novel target for glycolysis pathway inhibition, which may overcome HCC Sorafenib resistance.[15]

In the present study, we further found that the glycolysis pathway plays an important role in HCC patients' prognosis. When the cohort of HCC patients was divided into total-glycolytic (glycolytic + mixed type) and non-glycolytic (cholesterogenic + quiescent type) group, we found that the median OS of HCC patients in TCGA + ICGC (n = 512) was total-glycolytic: 1005 vs. non-glycolytic: 2486 days (P < .0001, Supplementary Fig. S8A). And the median OS of HCC patients in TCGA (n = 289) was: total-glycolytic: 765 vs. non-glycolytic: 2116 days (P < .0001, Supplementary Fig. S8B). This result showed that the HCC patients with high expression of glycolytic-related genes had a worse prognosis. Recently, several studies revealed that the glycolytic-related pathway played an important role in Sorafenib-resistant HCC. Wong et al provided a concept of the therapeutic potential of using 2-deoxyglucose, a glycolysis inhibitor, to reverse tumorigenicity and Sorafenib resistance mediated by protein arginine N-methyltransferase 6 (PRMT6) deficiency in HCC.[16] Liu et al reported that Gankyrin increases glucose consumption via activation of β-catenin/c-Myc to promote tumorigenesis, metastasis, and drug resistance in human HCC.[17] Furthermore, MPC plays a pivotal role in mitochondrial

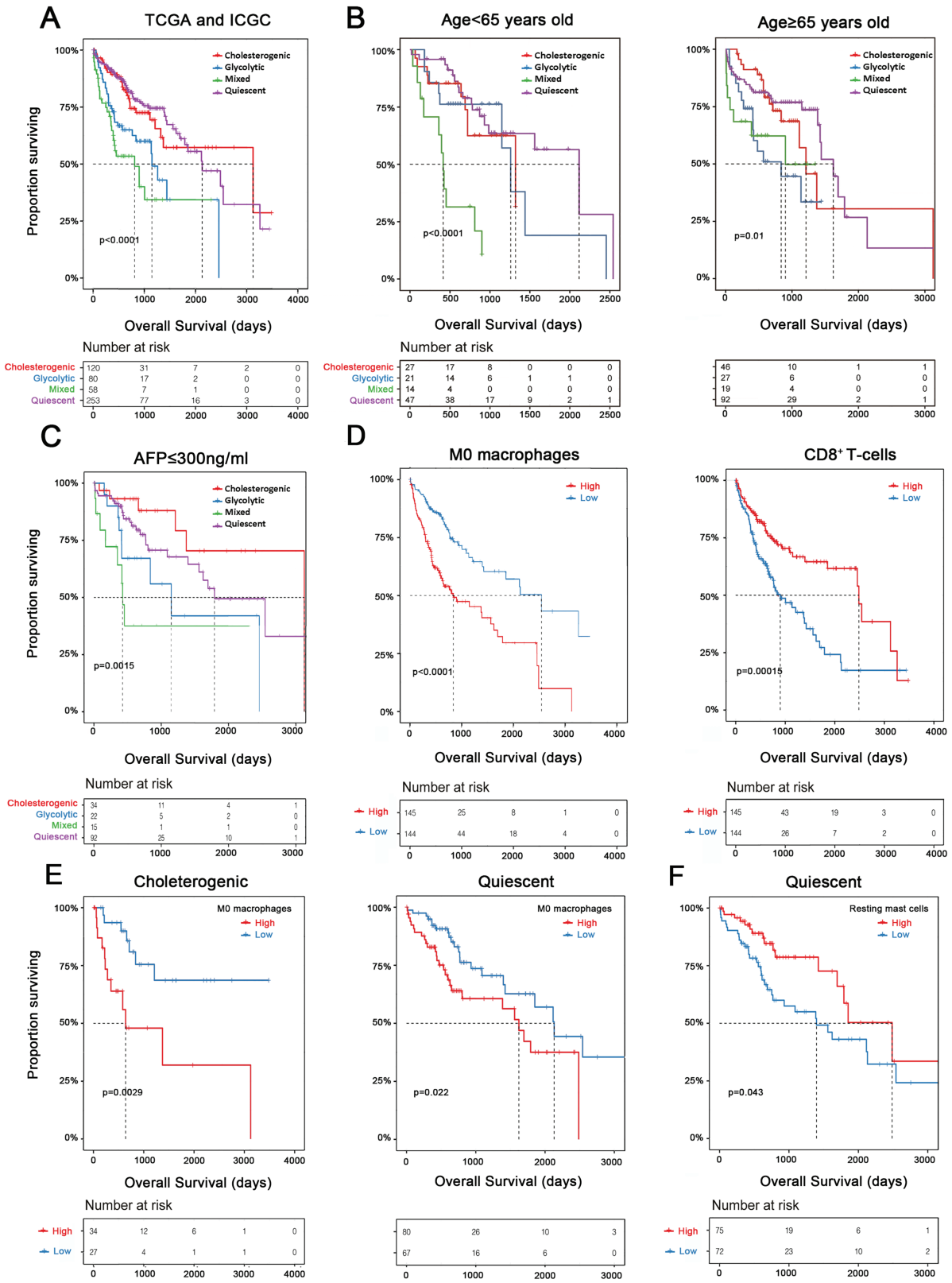

Figure 5. Association of tumor metabolic types, patients' ages, AFP levels, and the extent of tumor infiltration by immune cells with OS in patients with HCC. Prognosis is depicted with Kaplan-Meier curves: (**A**) for tumor metabolic subtype: in TCGA + ICGC (LIHC-US, LIRI-JP, and LICA-FR, $n = 511$), cholesterogenic versus glycolytic versus mixed versus quiescent type ($P < .0001$), (**B**) for HCC patients' age under 65 years in TCGA, similar results with (A) were obtained, the glycolytic subtype showed the highest mortality rate ($P < .01$) among patients older than 65 years, (**C**) prognosis is depicted for metabolic types in AFP level < 300 ng/mg ($P = .0015$) in TCGA, (**D**) for M0 macrophage: high versus low ($P < .0001$) in TCGA, for $CD8^+$ T cell: high versus low ($P = .00015$) in TCGA, (**E**) prognosis is depicted for metabolic types (cholesterogenic and quiescent type) in M0 macrophage distribution high and low (high vs. low: $P = .0029$ and .022, respectively), (**F**) prognosis is depicted for quiescent type in resting mast cell distribution high and low (high vs. low: $P = .043$) in TCGA. *P* values derived from log-rank tests.

carbohydrate oxidation and aerobic glycolysis in tumors. MPC transports pyruvate from the cytosol to the mitochondrial matrix, thereby regulating the tumor cell energy metabolism and inhibiting tumor progression.[18] In colon cancer, the *MPC1* and *MPC2* genes may increase mitochondrial pyruvate oxidation levels after metabolic reprogramming, thereby inhibiting tumor cell glycolysis levels and inhibiting cancer cell proliferation.[19] Ma et al found that MPC1 mRNA levels are significantly reduced in HCC,[20] which is concordant with our results. Therefore, studies on HCC-related MPC may reveal new tumor metabolic-related therapeutic approaches for HCC. These pieces of information showed evidence that HCC patients with high glycolytic metabolism may benefit from the treatments for the inhibition of glycolytic pathways.

Currently, studies on the effect of cholesterol metabolism on tumorigenesis and tumor progression are lacking. In ovarian cancer, cholesterol biosynthesis increases the mobility and invasive potential of ovarian cancer cells.[21] In the present study, *TTN* mutation correlated with cholesterol biosynthesis. Similarly, in esophageal squamous cell carcinoma lncRNA-TTN-AS1 promotes the proliferation and metastasis of cancer cells through miR133b/FSCN1.[22] This indicates that metabolism-related gene mutations may change the cholesterol biosynthesis process in HCC cells, and subsequently affect their invasiveness.

Immune cell tumor infiltration reflects the host's innate anti-tumor response. Tumor metabolic reprogramming may lead to a different metabolic status, which in turn may result in corresponding changes in the immune cell infiltration patterns, thus affecting patient prognosis.[23] In the present study, metabolic subgroups had differential immune cell infiltrates (Supplementary Fig. S9). Studies have shown that during aerobic glycolysis of cancer cells, $CD4^+$ T cells manifest higher activity,[24] thereby promoting tumor progression. Moreover, targeting the glycolysis pathway in tumor cells may restore monocyte activity and improve the anti-tumor immune response.[25] MAPK is an important pathway that mediates the relationship between metabolism and the immune system. *CSN5* promotes HCC metastasis by upregulating glycolysis, which leads to immune escape and worse prognosis.[26] We found that the distribution of immune cells in different metabolic subtypes was significantly different in HCC. Studies have suggested that B cells reshape anti-tumor immune responses and their infiltration is inversely correlated with tumor progression and can be used as an important prognostic factor.[27] Our analysis also showed a negative correlation between naïve B cell infiltration and HCC prognosis. Macrophage polarization is related to different metabolic characteristics associated with energy, iron, and fat metabolism.[28] A recent study presented that TAMs and M-MDSCs consume the most glucose per cell in the TME. We have a consistent result that M0 macrophages showed the highest infiltration in glycolytic subtype (P = .008, Fig. 3B). M0 is a type of non-polarized macrophage. Activated M1 and M2 macrophages have immunoregulatory functions of tumor suppression and tumor-promotion, respectively.[29] However, current research on M0 macrophages is limited. Some studies have found that the different infiltration patterns of the 3 types of macrophages correlate with different prognoses in breast cancer.[30] In the present study, M0 macrophage infiltration showed a negative impact on survival, in concordance with a previous study.[30] Behring et al found that the proportion of M0 macrophages in breast tumor tissues with *TP53* mutations is significantly increased, promotes tumor proliferation, and correlates with poor prognosis.[31] In ER-positive breast cancer and ovarian cancer, M0 macrophage infiltration negatively correlated with survival, confirming that it may gradually be recruited into tumor tissues and to promote tumor progression.[32,33] Furthermore, we found that M0 macrophage infiltration was negatively correlated with survival, which is concordant with the above conclusions.

Mast cells, another type of immune regulator, are largely inactive in HCC. IgE may activate resting into activated mast cells to negatively regulate tumoral growth. Resting (inactivated) mast cells may facilitate immune escape and thus favor tumor growth in HCC. Rohr-Udilova et al reported that resting mast cells were increased in HCC when compared to healthy livers, while activated mast cells were decreased.[34] In the present study, HCC patients with high resting mast cell infiltration exhibited a shorter survival in glycolytic subtypes. Therefore, M0 macrophages and resting mast cells may represent novel prognostic markers and potential HCC therapeutic targets.

DNA repair deficiency has emerged as a predictive biomarker of response to anti-PD-1 therapy.[35] Tumors with DNA mismatch repair (MMR) defects, such as MSI-high/MMR-deficient cancers, have an exceptionally high number of somatic mutations and are highly responsive to PD-1 blockade. Accordingly, pembrolizumab was approved for use in MSI-high/MMR-deficient solid tumors. In colon cancer, MSI induces PD-L1 expression in treated cells through tumor antigen-specific T-cell clones, while patients with MSS have lower PD-L1 expression in tumor cells, resulting in poor anti-PD-L1 treatment effect.[36] Since the incidence of MSI in HCC is low, the efficacy of PD-1/PD-L1 immunotherapy for HCC is not clinically ideal. Thus, to predict the effects of anti-PD-1 or anti-PD-L1 immunotherapy by using the MSI distribution in tumor cells is limited. However, the expression of PD-1 and PD-L1 among 4 metabolic subtypes showed significantly different distributions (Fig. 3C). Therefore, when choosing anti-PD-1 or anti-PD-L1 therapy for HCC, the metabolic type of the tumor should be considered. In addition, we found that glycolysis was positively correlated with AFP levels and could be used as a prognostic marker of HCC.

Conclusions

We identified distinct metabolic subtypes in HCC with differential association with prognosis and revealed an important correlation between the infiltration of multiple types of immune cells and clinical course within each metabolic subtype. This may lead to the study of metabolic immunology mechanisms, especially of the role of M0 macrophages which can be used as metabolic molecular therapeutic targets for HCC. The above may provide strong evidence for the future development of effective cancer metabolic immunotherapy strategies.

Limitations

This study is limited by the large sample set of the database involved in this project was derived from different human races and regions, which may have an impact on the data structure. Second, because some clinical data are missing in TCGA, ICGC, and GEO datasets, we could not compare

and verify our metabolic typing with Tokyo Scores and BCLC staging to reflect the advantages of metabolic typing. However, this is a sample analysis using extensively studied databases, and thus the above will not result in deviations in the results of our final analysis.

Funding

This study was supported by grants from Chongqing Overseas Chinese Returned Entrepreneurship and Innovation Foundation cx2022041 (PI: L.C.), Chongqing Natural Science Foundation CSTB2022NSCQ-MSX1460 (PI: L.C.), National Natural Science Foundation of China 81430063 (PI: X.W.L.), Natural Science Foundation of Chongqing CSTC2021JCYJ-MSXMX1095 (PI: X.X.W.), Science and Technology Innovation Commission Foundation of Shenzhen Grant JCYJ20190808120219139 (PI: X.L.W.), and Guangdong Provincial Key Laboratory of Regional Immunity and Diseases 2019B030301009 (PI: X.W.L.), and Guangdong Basic and Applied Basic Research Foundation Grant 2023A1515010323 (PI: X.L.W.).

Conflict of Interest

The authors indicated no financial relationships.

Author Contributions

Conception/design: X.W., T.M., C.R.F., L.C. Provision of study material or patients: X.W., Q.H., F.K., H.L., W.Z., X.L., L.C. Collection and/or assembly of data: X.W., T.M., Y.C., C.R.F. Data analysis and interpretation: X.W., T.M., S.F., C.R.F., X.L., L.C. Manuscript writing: X.W., C.R.F., X.L., L.C. Final approval of manuscript: All authors.

Data Availability

All data generated or analyzed during this study are included in this published article from the Cancer Genome Atlas (TCGA, https://portal.gdc.cancer.gov/), International Cancer Genome Consortium (ICGC, https://dcc.icgc.org/) and Gene Expression Om-nibus (GEO, https://www.ncbi.nlm.nih.gov/geo/)

Supplementary Material

Supplementary material is available at *The Oncologist* online.

References

1. Bray F, Ferlay J, Soerjomataram I, et al. Global cancer statistics 2018: Globocan estimates of incidence and mortality worldwide for 36 cancers in 185 countries. *CA Cancer J Clin*. 2018;68(6):394-424. https://doi.org/10.3322/caac.21492.
2. Zhong J-h, Ke Y, Gong W-f, et al. Hepatic resection associated with good survival for selected patients with intermediate and advanced-stage hepatocellular carcinoma. *Ann Surg*. 2014;260(2):329-340. https://doi.org/10.1097/sla.0000000000000236.
3. Pusapati RV, Daemen A, Wilson C, et al. Mtorc1-dependent metabolic reprogramming underlies escape from glycolysis addiction in cancer cells. *Cancer Cell*. 2016;29(4):548-562. https://doi.org/10.1016/j.ccell.2016.02.018.
4. Sukumar M, Liu J, Ji Y, et al. Inhibiting glycolytic metabolism enhances cd8+ T cell memory and antitumor function. *J Clin Invest*. 2013;123(10):4479-4488. https://doi.org/10.1172/JCI69589.
5. Ma C, Kesarwala AH, Eggert T, et al. NAFLD causes selective cd4(+) T lymphocyte loss and promotes hepatocarcinogenesis. *Nature*. 2016;531(7593):253-257. https://doi.org/10.1038/nature16969.
6. Kelly B, O'Neill LAJ. Metabolic reprogramming in macrophages and dendritic cells in innate immunity. *Cell Res*. 2015;25(7):771-784. https://doi.org/10.1038/cr.2015.68.
7. Zhang J, Baran J, Cros A, et al. International cancer genome consortium data portal—a one-stop shop for cancer genomics data. *Database: J Biolog Databases Curation*. 2011;2011:bar026. https://doi.org/10.1093/database/bar026
8. Roessler S, Jia HL, Budhu A, et al. A unique metastasis gene signature enables prediction of tumor relapse in early-stage hepatocellular carcinoma patients. *Cancer Res*. 2010;70(24):10202-10212. https://doi.org/10.1158/0008-5472.CAN-10-2607.
9. Li Y, Mo H, Jia S, et al. Comprehensive analysis of the amino acid metabolism-related gene signature for prognosis, tumor immune microenvironment, and candidate drugs in hepatocellular carcinoma. *Front Immunol*. 2022;13:1066773. https://doi.org/10.3389/fimmu.2022.1066773.
10. Ally A, Balasundaram M, Carlsen R, et al. Comprehensive and integrative genomic characterization of hepatocellular carcinoma. *Cell*. 2017;169(7):1327-1341.
11. Zhang C, Liu J, Liang Y, et al. Tumour-associated mutant p53 drives the Warburg effect. *Nat Commun*. 2013;4(1):2935. https://doi.org/10.1038/ncomms3935.
12. Harami-Papp H, Pongor LS, Munkácsy G, et al. Tp53 mutation hits energy metabolism and increases glycolysis in breast cancer. *Oncotarget*. 2016;7(41):67183-67195. https://doi.org/10.18632/oncotarget.11594.
13. Gao Q, Zhu H, Dong L, et al. Integrated proteogenomic characterization of HBV-related hepatocellular carcinoma. *Cell*. 2019;179(2):1240. https://doi.org/10.1016/j.cell.2019.10.038.
14. Charawi S, Just P-A, Savall M, et al. LKB1 signaling is activated in CTNNB1-mutated HCC and positively regulates β-catenin-dependent CTNNB1-mutated HCC. *J Pathol*. 2019;247(4):435-443. https://doi.org/10.1002/path.5202.
15. Deng L, Sun J, Chen X, et al. Nek2 augments sorafenib resistance by regulating the ubiquitination and localization of β-catenin in hepatocellular carcinoma. *J Exp Clin Cancer Res*. 2019;38(1):316.
16. Wong TL, Ng KY, Tan KV, et al. CRAF methylation by PRMT6 regulates aerobic glycolysis-driven hepatocarcinogenesis via ERK-dependent PKM2 nuclear relocalization and activation. *Hepatology*. 2020;71(4):1279-1296. https://doi.org/10.1002/hep.30923.
17. Liu R, Li Y, Tian L, et al. Gankyrin drives metabolic reprogramming to promote tumorigenesis, metastasis and drug resistance through activating beta-catenin/c-Myc signaling in human hepatocellular carcinoma. *Cancer Lett*. 2019;443:34-46. https://doi.org/10.1016/j.canlet.2018.11.030.
18. Taylor EB. Functional properties of the mitochondrial carrier system. *Trends Cell Biol*. 2017;27(9):633-644. https://doi.org/10.1016/j.tcb.2017.04.004.
19. Schell JC, Olson KA, Jiang L, et al. A role for the mitochondrial pyruvate carrier as a repressor of the Warburg effect and colon cancer cell growth. *Mol Cell*. 2014;56(3):400-413. https://doi.org/10.1016/j.molcel.2014.09.026.
20. Ma X, Cui Y, Zhou H, Li Q. Function of mitochondrial pyruvate carriers in hepatocellular carcinoma patients. *Oncol Lett*. 2018;15(6):9110-9116. https://doi.org/10.3892/ol.2018.8466.
21. Pampalakis G, Politi A-L, Papanastasiou A, Sotiropoulou G. Distinct cholesterogenic and lipidogenic gene expression patterns in ovarian cancer—a new pool of biomarkers. *Genes Cancer*. 2015;6(11-12):472-479. https://doi.org/10.18632/genesandcancer.87.
22. Lin C, Zhang S, Wang Y, et al. Functional role of a novel long noncoding RNA in esophageal squamous cell carcinoma progression

and metastasis. *Clin Cancer Res.: Off. J. Am. Assoc. Cancer Res*. 2018;24(2):486-498.
23. Zhang Q, Lou Y, Bai X-L, Liang T-B. Immunometabolism: a novel perspective of liver cancer microenvironment and its influence on tumor progression. *World J Gastroenterol*. 2018;24(31):3500-3512. https://doi.org/10.3748/wjg.v24.i31.3500.
24. Macintyre AN, Rathmell JC. Activated lymphocytes as a metabolic model for carcinogenesis. *Cancer Metab*. 2013;1:5. https://doi.org/10.1186/2049-3002-1-5.
25. Dietl K, Renner K, Dettmer K, et al. Lactic acid and acidification inhibit TNF secretion and glycolysis of human monocytes. *J Immunol*. 2010;184(3):1200-1209. https://doi.org/10.4049/jimmunol.0902584.
26. Huang M, Xiong H, Luo D, Xu B, Liu H. CSN5 upregulates glycolysis to promote hepatocellular carcinoma metastasis via stabilizing the HK2 protein. *Exp Cell Res*. 2020;388(2):111876. https://doi.org/10.1016/j.yexcr.2020.111876.
27. Sharonov GV, Serebrovskaya EO, Yuzhakova DV, et al. B cells, plasma cells and antibody repertoires in the tumour microenvironment. *Nat Rev Immunol*. 2020;20(5):294-307.
28. Biswas SK, Mantovani A. Orchestration of metabolism by macrophages. *Cell Metab*. 2012;15:432-437. https://doi.org/10.1016/j.cmet.2011.11.013.
29. Mantovani A, Marchesi F, Malesci A, Laghi L, Allavena P. Tumour-associated macrophages as treatment targets in oncology. *Nat Rev Clin Oncol*. 2017;14(7):399-416. https://doi.org/10.1038/nrclinonc.2016.217.
30. Raza AH, Leon C, Pharoah PDP, et al. Patterns of immune infiltration in breast cancer and their clinical implications: a gene-expression-based retrospective study. *PLoS Med*. 2016;13(12):e1002194.
31. Behring M, Vazquez AI, Cui X, et al. Gain of function in somatic TP53 mutations is associated with immune-rich breast tumors and changes in tumor-associated macrophages. *Mol Genet Genomic Med*. 2019;7(12):e1001. https://doi.org/10.1002/mgg3.1001.
32. Liu R, Hu R, Zeng Y, Zhang W, Zhou H-H. Tumour immune cell infiltration and survival after platinum-based chemotherapy in high-grade serous ovarian cancer subtypes: a gene expression-based computational study. *EBioMedicine*. 2020;51:102602. https://doi.org/10.1016/j.ebiom.2019.102602.
33. Zhang SC, Hu ZQ, Long JH, et al. Clinical implications of tumor-infiltrating immune cells in breast cancer. *J Cancer*. 2019;10(24):6175-6184. https://doi.org/10.7150/jca.35901.
34. Rohr-Udilova N, Klinglmüller F, Schulte-Hermann R, et al. Deviations of the immune cell landscape between healthy liver and hepatocellular carcinoma. *Sci Rep*. 2018;8(1):6220. https://doi.org/10.1038/s41598-018-24437-5.
35. Le DT, Durham JN, Smith KN, et al. Mismatch repair deficiency predicts response of solid tumors to pd-1 blockade. *Science (New York, NY)*. 2017;357(6349):409-413.
36. Luchini C, Bibeau F, Ligtenberg MJL, et al. ESMO recommendations on microsatellite instability testing for immunotherapy in cancer, and its relationship with PD-1/PD-l1 expression and tumour mutational burden: a systematic review-based approach. *Ann Oncol: Off J Eur Soc Med Oncol*. 2019;30(8):1232-1243.